A Journal of the Gesellschaft Deutscher Chemiker

Angewandte International Edition Chemie

GDCh

www.angewandte.org

Accepted Article

Title: Multiphoton-driven Photocatalytic Defluorination of Persistent Perfluoroalkyl Substances and Polymers by Visible Light

Authors: Yuzo Arima, Yoshinori Okayasu, Daisuke Yoshioka, Yuki Nagai, and Yoichi Kobayashi

To be cited as: *Angew. Chem. Int. Ed.* **2024**, e202408687

Link to VoR: https://doi.org/10.1002/anie.202408687

WILEY VCH

10.1002/anie.202408687

RESEARCH ARTICLE

Multiphoton-driven Photocatalytic Defluorination of Persistent Perfluoroalkyl Substances and Polymers by Visible Light

Yuzo Arima,[a] Yoshinori Okayasu,[a] Daisuke Yoshioka,[a] Yuki Nagai,[a] and Yoichi Kobayashi*[a]

[a] Y. Arima, Dr. Y. Okayasu, D. Yoshioka, Dr. Y. Nagai, Prof. Y. Kobayashi
Department of Applied Chemistry, College of Life Sciences
Ritsumeikan University
1-1-1 Nojihigashi, Kusatsu, Shiga 525-8577 (Japan)
ykobayas@fc.ritsumei.ac.jp

Supporting information for this article is given via a link at the end of the document.

Abstract: Perfluoroalkyl substances (PFASs) and fluorinated polymers (FPs) have been extensively utilized in various industries, whereas their extremely high stability poses environmental persistence and waste treatment. Current decomposition approaches of PFASs and FPs typically require harsh conditions such as heating over 400°C. Thus, there is a pressing need to develop a new technique capable of decomposing them under mild conditions. Here, we demonstrated that perfluorooctanesulfonate (PFOS), known as a "persistent chemical," and Nafion, a widely utilized sulfonated FP for ion-exchange membranes, can be efficiently decomposed into fluorine ions under ambient conditions via the irradiation of visible LED light onto semiconductor nanocrystals (NCs). PFOS was completely defluorinated within 8-h irradiation of 405-nm LED light, and the turnover number of the C–F bond dissociation per NC was 17200. Furthermore, 81% defluorination of Nafion was achieved for 24-h light irradiation, demonstrating the efficient photocatalytic properties under visible light. We revealed that this decomposition is driven by cooperative mechanisms involving light-induced ligand displacements and Auger-induced electron injections via hydrated electrons and higher excited states. This study not only demonstrates the feasibility of efficiently breaking down various PFASs and FPs under mild conditions but also paves the way for advancing toward a sustainable fluorine-recycling society.

Introduction

Perfluoroalkyl substances (PFASs) and fluorinated polymers (FPs) exhibit excellent heat resistance, chemical resistance, insulating properties, and interfacial characteristics, rendering them indispensable in various industrial fields. However, the extremely strong carbon–fluorine (C–F) bond in these compounds leads to various environment-related challenges. For example, PFASs typically exhibit notable environmental persistence, and certain PFASs such as perfluorooctane sulfonate (PFOS) and perfluorooctanoic acid (PFOA) are highly bioaccumulative. Moreover, waste treatment of fluorinated compounds is challenging because the hydrogen fluoride generated by the combustion of fluorinated compounds deteriorates incinerators.[1,2]

Several techniques have been reported to decompose PFAS into recyclable fluoride ions, including oxidation using strong oxidants such as peroxydisulfuric acid and ultraviolet-C (UVC) irradiation (wavelength below 260 nm) using a mercury lamp under high temperature and pressure.[3–13] Fluorine ions can be converted to calcium fluoride, which is a natural source of fluorine, and therefore, fluorine-recycling can be achieved. However, the use of mercury lamps as a light source is becoming less feasible owing to regulatory constraints imposed by the Minamata Convention on Mercury. A recent study demonstrates that perfluorooctanoic acid (PFOA) can be mineralized under strong basic conditions at 100°C.[13] However, such mild conditions are not suitable for the decomposition of more stable PFASs, such as PFOS and FPs. Despite the widespread use of FPs in diverse industrial applications, their recycling rate remains low, and many of them are subjected to landfill burial.[14] Therefore, it is necessary to develop a method to decompose extremely stable PFAS under mild conditions to address the multifaceted social issues linked with PFAS and to contribute to the realization of a sustainable fluorine-recycling society.

In recent years, nonlinear optical processes that could be induced by weak incoherent light have been extensively investigated,[15–22] and these have been applied to various organic photocatalytic reactions.[20,23–27] Specifically, long-lived transient states of organic molecules and metal complexes generated by LED light are further photoexcited to proceed with chemical reactions requiring higher photon energy than incident light energy. In addition to organic compounds, advanced photocatalytic reactions have also been reported using inorganic nanostructures. In particular, semiconductor nanocrystals (NCs) have a high absorption coefficient, and multiple excitons can be generated relatively easily within a NC. When multiple excitons interact, a process by which one exciton uses its recombination energy to transition to a higher excited state, called Auger recombination, occurs, and a highly excited electron or hole is produced.[28,29] The highly excited electronic states are generally thermally deactivated quickly. On the other hand, if the highly excited electrons can be extracted efficiently, this can be an extremely effective upconversion reaction system.

Klimov and Oron groups have achieved upconversion using Auger recombination from CdSe to CdS moieties in these

10.1002/anie.202408687
WILEY VCH

RESEARCH ARTICLE

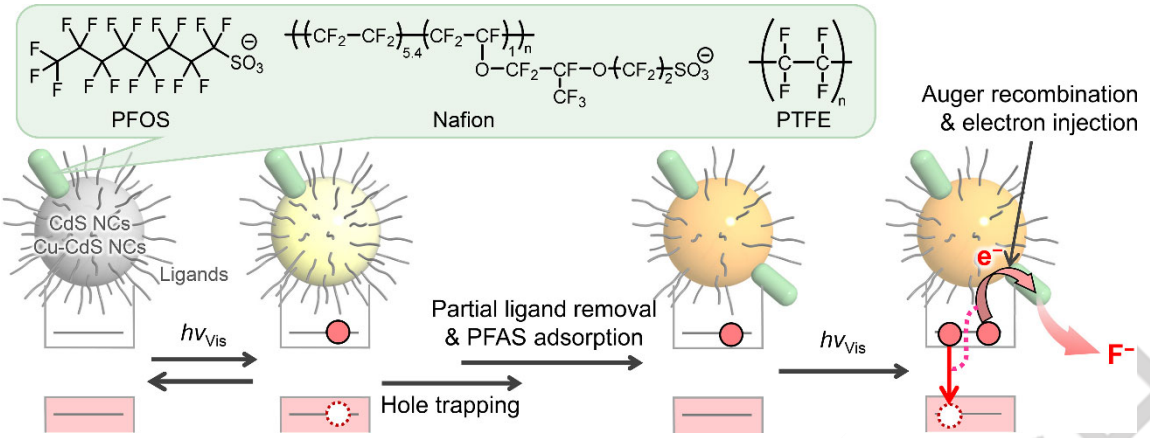

Figure 1. Plausible reaction mechanism of visible-light-induced defluorination of PFAS by semiconductor NCs.

CdS/CdSe heteronanostructures.[30–32] Son and Gamelin groups have achieved energy transfer upconversion similar to Auger recombination using Mn-doped CdS NCs.[33–36] More recently, Krauss and Weix *et al.*[37,38] demonstrated elimination reactions of halogens of aryl halides using CdS NCs. On the other hand, their reactions are limited to the decomposition of allyl halide and chloroacetic acid, which are relatively easy to reduce. Moreover, most systems are constrained to photoredox reactions in organic solvents, and there are few examples in aqueous solutions except for research on hydrogen evolutions probably because water induces various side reactions including the decomposition of catalysts.

In this study, we demonstrate that PFOS and FPs can be efficiently decomposed to fluorine ions in aqueous solutions at room temperature and atmospheric pressure through the irradiation of visible LED light onto CdS and copper-doped CdS (Cu-CdS) NCs. While visible light energy is typically insufficient to break the strong C–F bonds, we overcome this limitation by Auger recombination. Typically, electrons in the higher state tend to relax to the lowest excited state via nonradiative relaxation. However, a fraction of these electrons is either directly transferred to PFASs when adsorbed onto the NC surface or is released into the medium, forming hydrated electrons. Hydrated electrons possess a reduction potential (−2.9 V vs standard electron electrode (SHE)) exceeding that of metallic sodium,[39,40] and therefore can be used to decompose PFASs through reduction reactions. In colloidal NC systems, trapping of a photogenerated hole by hole scavengers likely extends the lifetime of the conduction band electron (Fig. 1), which facilitates the absorption of another photon to produce a negative trion (a three-carrier state composed of two electrons and a hole). Simultaneously, photoirradiation promotes the desorption of organic ligands from the NC surface, which in turn enhances the adsorption of PFAS onto the NC surface. Consequently, the efficient decomposition of PFAS occurs through cooperative multiphoton processes involving light-induced ligand displacements and Auger-induced electron injections via hydrated electrons and the higher excited states of NCs. If a negative trion is replaced with a positive trion (a three-carrier state composed of one electron and two holes), highly oxidative states can also be produced. This advanced decomposition technique can be applied to decompose other persistent chemicals under mild conditions, contributing to the realization of a sustainable fluorine-recycling society.

Results and Discussion

CdS and Cu-CdS NCs were synthesized in aqueous solutions using 3-mercaptopropionic acid (MPA), following a reported protocol.[41] X-ray diffraction (XRD) measurements showed that the crystal structures of CdS and Cu-CdS NCs corresponded to zincblende structures, regardless of the amount of Cu (Fig. S1 in the supporting information (SI)). The average diameters of CdS NCs were estimated based on the excitonic absorption peak in the steady-state absorption spectra,[42] while those of Cu-doped CdS NCs were estimated by the peak width of XRD patterns. The atomic ratio of Cu per Cd ranged from 0–12%, as confirmed by X-ray fluorescence spectroscopy. Cu doping did not introduce XRD peaks related to impurities or optical absorption tails in the longer

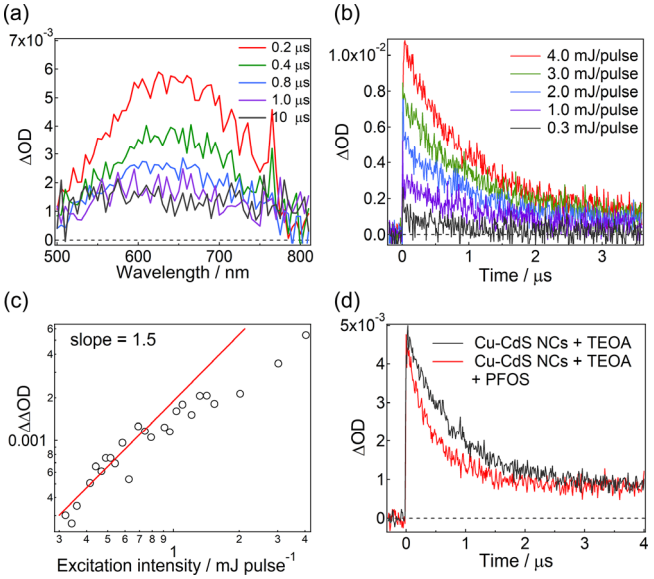

Figure 2. (a) Transient absorption spectra of 12% Cu-CdS NCs excited with a 355-nm nanosecond laser pulse (4.0 mJ pulse^{-1}). (b) Transient absorption dynamics at 700 nm under different excitation intensities. (c) Amplitude of the submicrosecond decay component (ΔΔOD) as a function of excitation intensity. (d) Reaction of the hydrated electron with PFOS in the presence of triethanolamine (TEOA).

wavelength, indicating the absence of the Cu_xS domain. The aqueous solutions of MPA-capped CdS and Cu-CdS NCs exhibited absorption below 450–500 nm, depending on the size and composition (Fig. S3). Cu doping slightly shifted the absorption spectra to a longer wavelength, probably because of the formation of midgap states dominated by Cu(3d) above the valence band.[43]

To investigate the photogenerated transient species, we conducted laser flash photolysis measurements using a 355-nm nanosecond laser pulse. As an example, the transient absorption spectra and dynamics of the aqueous solution of 12% Cu-CdS NCs are shown in Fig. 2. Cu-CdS NCs do not show the defect emission of CdS NCs on microsecond timescales, which interferes with the observation of the transient species, whereas similar photocatalytic reactions were observed in Cu-CdS and CdS NCs. Results of CdS NCs measured by the randomly interleaved pulse train (RIPT) method, which removes the emission component by taking the difference for each laser shot, are shown in Fig. S4. Immediately after the excitation, a broad positive transient absorption band was observed at 640 nm (Fig. 2a). The transient species decayed with a time constant of 0.90 μs (Fig. 2b). Moreover, the signal increased nonlinearly with increase in the excitation intensity (Fig. 2c). The spectral shape, lifetime, and nonlinear dependence indicated that the short-lived transient species originated from a hydrated electron generated by Auger recombination.[44] Because the photon flux density was insufficient for a simultaneous two-photon process, the hydrated electron was produced by the stepwise two-photon process. The quantum yield for hydrated electron generation was estimated to be 1.5×10^{-2} when the excitation intensity was 4.0 mJ pulse^{-1} (details can be found in the SI). The transient signal associated with the hydrated electron decayed faster (0.46 μs) upon the addition of PFOS to the solution (~6.2×10^{-4} M, Fig. 2d). On the other hand, the emission decay of CdS NCs did not change at all by the addition of PFOS to the solution (Fig. S10). These results suggest that PFOS reacted with the hydrated electron generated by Auger recombination.

Solutions for photocatalytic reactions were prepared by adding CdS NCs, PFOS, and triethanolamine (TEOA, as a hole scavenger) to milli-Q water and N_2 bubbling (see Methods and Table S1 for details). In a typical photocatalytic reaction, 0.8 mg of CdS NCs (equivalent to 1.0×10^{-8} mol for 3.4-nm CdS NCs), PFOS (0.65 mg, 1.2×10^{-6} mol), and TEOA (20 mg, 1.3×10^{-4} mol) were added to 1.0 mL of milli-Q water. Then the sample was mixed by sonication, stirring for 10 min, and nitrogen bubbling for 30 min in the 10-mm quartz cuvette. 405-nm LED light was irradiated into the solution to investigate the decomposition of PFOS (Fig. S5). After the light irradiation, the solution was centrifuged (15000 rpm, 5 min) and decantated. The decomposition process of PFOS was monitored by 19-fluorine nuclear magnetic resonance (^{19}F-NMR) spectroscopy, ion chromatography, and liquid chromatography-mass spectrometry (LC-MS) measurements. Based on the concentration of fluorine ions in the aqueous solution, the defluorination efficiency (*overall* deF%) was calculated by the following equation,

$$overall\ \mathrm{deF\%} = \frac{[\mathrm{F^-}]}{n[\mathrm{PFAS}]_0} \times 100\ (\%) \qquad (1)$$

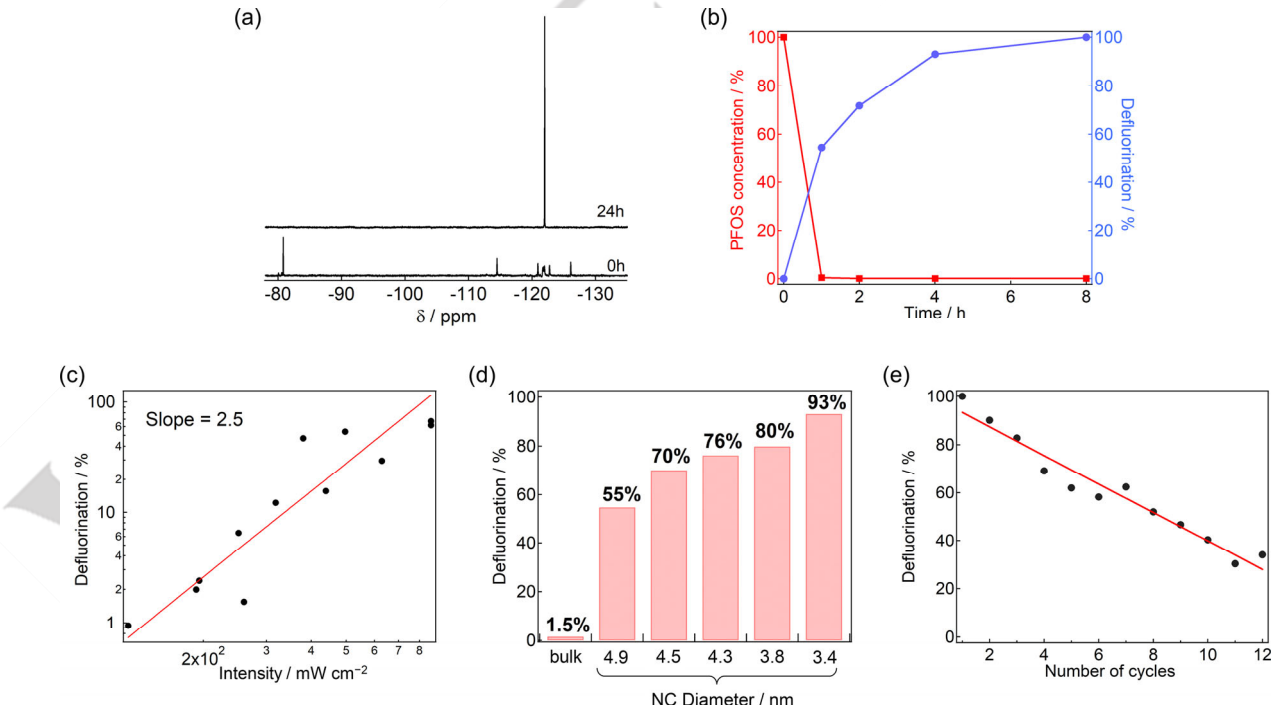

Figure 3. (a) ^{19}F-NMR spectra of the aqueous reaction solution before and after 405-nm light irradiation (830 mW cm^{-2}). (b) Time profiles of PFOS concentration in the reaction solution and overall defluorination efficiency of the reaction solution. Dependence of the overall defluorination efficiency on (c) irradiation power, and (d) NC diameter. (e) Repeated decomposition experiments using the same CdS NCs. One cycle includes (1) N_2 bubbling of the reaction solution for 30 min, (2) irradiation of 405-nm LED light for 12 h, (3) centrifugation and removal of the supernatant, and (4) addition of 1.0 mL of the aqueous solution containing PFOS (1.2×10^{-6} mol) and TEOA (1.3×10^{-4} mol). The defluorination efficiency was measured for the solution subjected to centrifugation. Details of the experimental conditions can be found in the Materials and Methods section in the supporting information.

10.1002/anie.202408687

where $[F^-]$, n, and $[PFAS]_0$ are the concentration of fluorine ions, the number of C–F bonds per molecule (17 and 3460 for PFOS and Nafion, respectively), and the initial concentration of PFOS and the sulfonated polymer, respectively.

The peaks of the ^{19}F-NMR spectrum of the reaction solution (deuterated water was used only for NMR measurements) before light irradiation originates from PFOS (Fig. 3a). After 405-nm light irradiation (830 mW cm^{-2}) for 24 h, only an intense sharp peak at −121 ppm was observed, attributable to the fluorine ion. This observation shows that PFOS can be decomposed to fluorine ions by visible-light irradiation.

The defluorination efficiency (*overall* deF%) depends on the amounts of NCs and TEOA (Fig. S8), and the optimized *overall* deF% were 55%, 70–80%, and 100% for 1-, 2-, and 8-h light irradiation, respectively (Fig. 3b). We have confirmed that when the experiment was repeated multiple times under the same conditions at the same time, the variation in defluorination efficiency was approximately within ±~5%. The overall defluorination efficiency gradually increased with the increase in the irradiation period. On the other hand, the concentration of PFOS in the solution quickly dropped to almost zero only after 1-h light irradiation. The concentration of PFOS was <0.1% after 8-h light irradiation. It indicates that PFOS is quickly converted to other PFASs by defluorination and/or adsorbed on the surface of NCs (*Vide infra*). The quantum efficiency of C–F bond dissociations was determined to be 2.0 × 10^{-3} using the *overall* deF% after 1-h irradiation of 405-nm LED light (see the SI for details). Considering that the quantum efficiency for the generation of hydrated electrons was 1.5 × 10^{-2} under the nanosecond laser pulse excitation, the observed quantum efficiency for C–F bond dissociations using LED light appears remarkably high. This is probably due to the contribution of the direct electron transfer from higher excited states to the decomposition of PFOS in addition to the reaction with hydrated electrons. Although lifetimes of higher excited states are generally extremely short, the electron transfer from the higher excited states is possible if the substrate is in close proximity. In addition, the higher excited state generated by Auger recombination in the present CdS NCs (~−3.5 V vs SHE) is even more reductive than those of hydrated electrons. Therefore, reactions of higher excited states with PFOS are plausible if PFOS is directly adsorbed on the NC surface. Similar photocatalytic behaviors were observed with Cu-CdS NCs (Fig. S9). Although Cu doping may help extend the lifetime of the excited state, it might also increase the deactivation pathways for the excited electrons.

The *overall* deF% after 4-h light irradiation exhibited a nonlinear dependence on the excitation intensity, even with LED light (Fig. 3c, with a slope of 2.5). This result indicates that multiphoton processes are involved in the PFOS decomposition. The reduction potential of the conduction band of CdS (−0.9 V vs. SHE)[45] is lower than that of PFOS (−1.3 V vs. SHE)[5] even taking the pH and quantum size effect into account (−1.19 V vs. SHE).[45,46] Moreover, the emission decay of CdS NCs was not affected at all by the presence of PFOS (Fig. S10). These results strongly suggest that hydrated electrons and higher excited states generated by Auger recombination are involved in PFOS decomposition. The defluorination efficiency increased with decreasing NC diameter (Fig. 3d), and the defluorination efficiency substantially decreased in commercial bulk CdS although the primary particle size estimated by the linewidth of X-ray diffractions was 7.4 nm. The efficient decomposition reaction in smaller NCs is consistent with the fact that Auger recombination is enhanced in a strong confinement regime and the rate of Auger recombination increases with smaller NC size in addition to the larger surface-to-volume ratio in smaller NCs [28,47]. Moreover, the slope of the power dependence in this study exceeded 2, whereas the experimentally observed slope of the power dependence of two-photon processes is typically below 2 owing to the involvement of other optical processes and reabsorption by photogenerated species. It suggests that another photochemical process, i.e, three-photon processes in total, is involved in PFOS decomposition, as discussed later.

The defluorination efficiency substantially decreased without hole scavengers (TEOA), owing to the photocorrosion of CdS NCs (Fig. S11). In addition, the presence of molecular oxygen resulted in low defluorination efficiency (Fig. S11). Several researchers have suggested that hydroxyl radicals generated by photogenerated holes are involved in PFAS decomposition [48]. Although we detected hydroxyl radicals with a hydroxyl radical probe (terephthalate anion) upon light irradiation, the generation of hydroxyl radicals was suppressed by the addition of TEOA (Fig. S12). These results suggest that the photogenerated holes mainly lead to photocorrosion and do not contribute to the decomposition of PFOS in this system.

During the photocatalytic reactions, the solution color changed from yellow to brown or dark brown by light irradiation (Fig. S13), which could be ascribed to the photocharging and the generation of metal cadmium (discussed in detail later). Moreover, the solution gradually became turbid and the precipitate was observed within 2-h light irradiation, suggesting that the initial surface ligands of the NCs were desorbed or deteriorated by light irradiation. The XRD pattern and peak width of the precipitates indicated that the diameter of CdS NCs remained constant despite the photochemical reactions (Fig. S14b). Fourier transform infrared (FTIR) spectra show that MPA was replaced with other organic molecules probably ascribed to TEOA and its photoproducts (Fig. S14a). These results indicate that organic molecules on the surface of NCs dynamically change upon visible light, whereas NCs more or less retain their sizes.

PFOS can coordinate with the surface Cd atoms by its sulfonate group. Because the NC surface covered with TEOA and its decomposed products is presumably positively charged, the ligand exchange upon light irradiation may facilitate the adsorption of negatively charged PFOS through electrostatic interactions. On the other hand, we did not observe induction periods in the time profiles of the defluorination efficiency of the reaction solution (Figure 3b). It may indicate that the exchange of surface molecules progresses relatively quickly.

The precipitated CdS NCs could be reused to decompose PFOS over more than 12 cycles (Fig. 3e), although the *overall* deF% gradually decreased. Each cycle involved (1) N_2 bubbling of the reaction solution for 30 min, (2) irradiation of 405-nm LED light for 12 h, (3) centrifugation and decantation of the supernatant, and (4) addition of 1.0 mL of the aqueous solution containing

10.1002/anie.202408687

RESEARCH ARTICLE

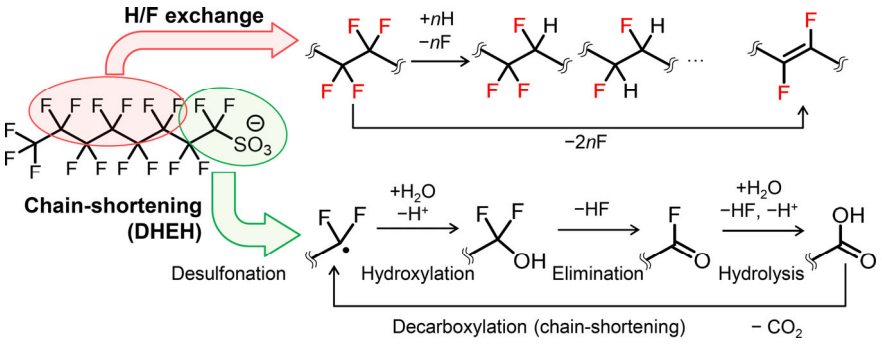

Figure 4. Plausible decomposition mechanism of PFOS by visible light irradiation to CdS NCs.

PFOS (1.2×10^{-6} mol) and TEOA (1.3×10^{-4} mol). The ratio of CdS NC and PFOS per cycle was 1:122.2, with each PFOS molecule containing 17 C–F bonds. The turnover number of C–F bond dissociation per CdS NC was calculated to be 17200 from the line exploration. The concentration of cadmium (II) ions dissolved in the solution was 3 ppm after the first cycle, and varied between 6–46 ppm (the average was 13 ppm except for outliers) depending on the experimental conditions (Fig. S15), which corresponds to 1–7% of the remained CdS NCs. The large deviation of the Cd concentration may be due to insufficient removal of molecular oxygen because molecular oxygen promotes photocorrosion. The slight photocorrosion is consistent with the gradual decrease in the *overall* deF% by repeating the photocatalytic reactions.

Scanning transmission electron microscopy (STEM) measurements revealed that the shape and crystallinity were preserved after 1-h light irradiation (Fig. S16), which is consistent with the results of XRD measurements (Fig. S14b). Moreover, elemental mapping revealed that F atoms were observed around CdS NCs, whereas they were hardly observed in the sulfur layers probably generated by the dissolution of CdS NCs (Fig. S17). It indicates that the decomposition of PFOS mainly proceeds on the surface of CdS NCs.

Previous reports on PFOS decomposition by UVC light using a mercury lamp highlighted two potential mechanisms for PFOS decomposition: H/F exchange and chain-shortening (Fig. 4).[3,6] The latter mechanism is known as decarboxylation (desulfonation as a first step in this case)-hydroxylation-elimination-hydrolysis (DHEH) mechanism. LC-MS analyses before light irradiation suggested that the commercial linear PFOS used in this study contained several branched PFASs, such as perfluoroheptanesulfonate (PFHpS, m/z = 449), perfluorohexanesulfonate (PFHxS, m/z = 399), and a small amount of PFOA (m/z = 413, Fig. S18–S30). After light irradiation for 1 h, the signals associated with PFOS substantially decreased, and multiple peaks originating from molecules with one or two F atoms of PFOS replaced with H atoms were observed (m/z = 481 and 463, Fig. S31–S57). In addition, several peaks associated with molecules, where several even numbers of F atoms were abstracted and some of C–C bonds were converted to double or triple bonds, were observed (such as m/z = 461, 443, 425, 407, 405). These results suggested that the H/F exchange reaction occurred during the decomposition of PFOS.

On the other hand, only products with fewer than three substituted hydrogen atoms were observed by H/F exchange, and the most defluorinated anion detected even after prolonged light irradiation was $C_8F_{10}H_3SO^{3-}$ (m/z = 369). Moreover, the signals associated with the anions generated by H/F exchange reactions decayed with increasing irradiation time. Considering the near-unity defluorination efficiency in this system, another defluorination mechanism, i.e., the chain-shortening reaction likely occurred through visible-light irradiation. However, peaks derived from shorter-chain carboxylate anions, including trifluoroacetic acetate, were not observed even in the matrix-assisted laser desorption/ionization-time-of-flight mass spectrometry (MALDI-TOF MS) measurements of the solution after the reaction (Fig. S105–S108). Shorter-chain carboxylate PFASs are usually more reactive than PFOS and could be readsorbed on the NC surface, where further defluorination reactions would proceed. Therefore, the absence of these small PFASs may indicate the efficient progression of DHEH reactions, resulting in the complete decomposition of PFOS to fluorine ions.

Because hydrated electrons and higher excited states are short-lived, PFOS and NCs being in close proximity, i.e., the adsorption of PFOS onto the surface of NCs, is crucial for an efficient decomposition reaction. The decrease in the ^{19}F-NMR signals of PFOS dissolved in the aqueous solution by the addition of CdS NCs indicates that PFOS was promptly adsorbed onto the surface of NCs in the solution (Fig. 5a). LC-MS analyses revealed that 21% of PFOS were adsorbed on the surface of NCs 5 min after the addition of CdS NCs to the solution for photocatalytic reactions (Fig. S109). Prior studies have shown that coordinated ligands are displaced under light irradiation, and the readsorption of displaced ligands requires more than several seconds[49,50]. The origin of the photoinduced ligand displacement was revealed to be the dramatic decrease in the Coulomb force between the NC moiety and the ligand by photoinduced electron transfer.[50] In the present experiment, despite MPA being coordinated to the NC surface before the reaction, TEOA and its likely decomposed products were primarily observed on the NC surface after the reaction (Fig. S14a). It suggests that the organic molecules on the NC surface dynamically transform under light irradiation. The photoinduced ligand displacement was observed through proton-NMR (^{1}H-NMR) spectroscopy of the deuterated solution of MPA-capped CdS NCs (Fig. 5b). Broad peaks at 2.2–3.5 ppm before light irradiation were attributable to the MPA coordinated on the surface of NCs, while several sharp peaks were ascribed to

10.1002/anie.202408687

weakly bound or free MPA. The sharp peaks associated with free MPA increased upon irradiation of 405-nm LED light (830 mW cm^{-2}) for 5 min. Moreover, the sharp peaks decreased again 1 h after light irradiation. These results indicated that MPA ligands were displaced by light irradiation, and the displaced MPA gradually readsorbed onto the NCs. This ligand displacement most probably facilitates the adsorption of PFOS onto the surface of NCs and accelerates the photodecomposition of PFOS. The timescale of the observed reaction was considerably slower than that reported previously, possibly because the extended duration of light irradiation promoted the persistence of displaced ligands.

The reaction between PFOS and hydrated electrons, as well as higher excited states, should be completed within several microseconds. If the ligand displacement reaction plays a pivotal role in driving PFOS decomposition, the decomposition efficiency is expected to be affected by the non-light irradiation periods during the light irradiation even when the total irradiation period is the same. To elucidate the relationship between ligand displacement on the NC surface and PFOS decomposition, we measured the *overall* deF% under different irradiation conditions. Specifically, the light was irradiated for 10 s and paused for specified intervals (10 s, 1 min, and 2 min, as illustrated in Fig. 5c). This cycle was repeated to achieve an equivalent total irradiation duration as that of continuous irradiation for 1 h. Moreover, we monitored the solution temperature because it changes based on the duration of irradiation.

Following continuous light irradiation for 1 h, the *overall* deF% was 56% and the solution temperature after the light irradiation was 311 K. The decrease in the solution temperature to 296 K under the same irradiation condition led to a decrease in the *overall* deF% to 41%. In contrast, 10-second irradiation intervals resulted in a decrease in the *overall* deF% to 32%, even though the solution temperature was 300 K. As the interval increased to 1 min, the *overall* deF% further decreased to 11% at 298 K, whereas the *overall* deF% maintained at 296 K with a 2-min interval. These observations indicate the involvement of another chemical reaction occurring on timescales of seconds to tens of seconds in PFOS decomposition. Moreover, the observed adsorption of displaced ligands, requiring several seconds to tens of seconds, and the slope of excitation dependence exceeding 2 highlight the significance of light-induced ligand desorption/adsorption reactions in PFOS decomposition. Once a ligand is desorbed, PFOS can coordinate with the NC surface, facilitating its efficient degradation. These results collectively suggest that the interplay between ligand desorption, PFOS adsorption, and nonlinear photoreaction processes plays a pivotal role in the efficient decomposition of PFOS under visible light (Fig. 5d).

Metal cadmium is expected to be generated upon light irradiation. Thus, its role in the defluorination reaction was experimentally studied. The generation of the metal cadmium on the NC surface was confirmed by a change in solution color from yellow to dark brown upon light irradiation.[51] The dark brown

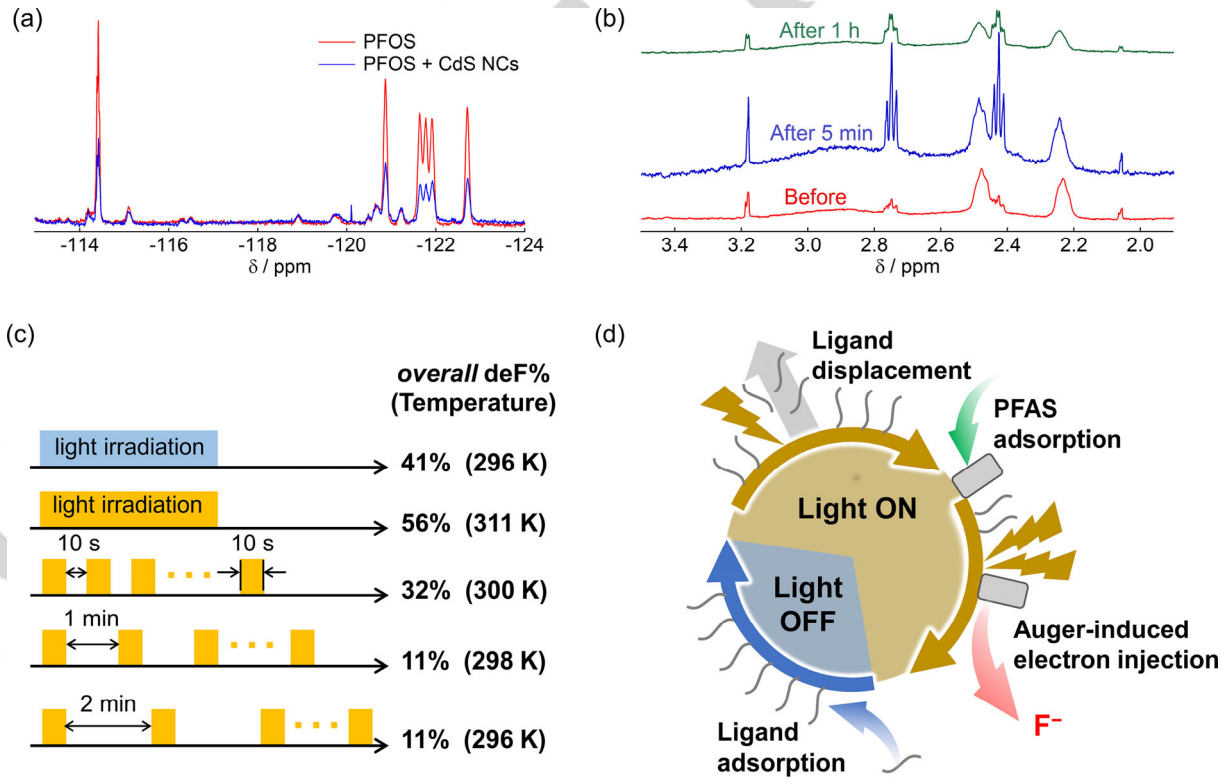

Figure 5. (a) ^{19}F-NMR spectra of the aqueous solution of PFOS (1.2×10^{-3} M) before and after the addition of CdS NCs (2.7×10^{-4} M). (b) ^{1}H-NMR spectra of CdS NCs before and after light irradiation (405 nm, 830 mW cm^{-2}) for 5 min. Broad peaks indicate MPA ligands coordinated to the surface of NCs, while sharp peaks correspond to free MPA. (c) Schematics of light irradiation conditions, along with overall defluorination efficiency (*overall* deF%) and temperature of the reaction solution upon completion of light irradiation. (d) Plausible mechanism underlying the relationship between ligand displacement and PFOS decomposition.

color persisted throughout the reaction and gradually faded over a day after the termination of light irradiation. This long lifetime of metal cadmium is inconsistent with the fact that the transient species contributing to the defluorination reaction are generated within a few seconds or tens of seconds. Notably, although the formation of metal cadmium was promoted by the addition of cadmium precursors ($CdCl_2$ or $Cd(CH_3COO)_2$), the *overall* deF% decreased (remaining nearly constant for $Cd(CH_3COO)_2$) with the addition of these precursors (Fig. S110 and S111). These results indicate that metal cadmium was not involved in the main pathways of defluorination reactions. Although sulfide ions and their byproducts may be potential photodegradation products of CdS, the reaction efficiency did not improve even after the addition of sulfide ions (Fig. S112). This result suggests that sulfur ions and their byproducts were not likely to be involved in the reaction. This result is consistent with the results of STEM measurements that the F atoms were hardly observed in the photogenerated sulfur layers.

This defluorination method can be applied to perfluorinated alkyl polymers such as Nafion (Fig. 1). Nafion is widely used as an ion-exchange membrane in electrolysis and batteries. For the powder form of Nafion, where the sulfonate groups are $-SO_2F$, the *overall* deF% under the same experimental condition with PFOS was at most 1.8% after irradiation for 24 h (Fig. S112). When the same reaction was performed with Nafion dispersed in a water/ethanol mixture solution by saponification, where the sulfonate groups are $-SO_3^-$, the *overall* deF% dramatically increased to 81% over 24-h light irradiation (Fig. S113 and S114). These results demonstrated that nonlinear photoreactions of semiconductor NCs can efficiently decompose perfluoroalkyl polymers, emphasizing the significance of proximity between the NCs and the substrate for the reaction. Furthermore, polytetrafluoroethylene (PTFE) powder can also be defluorinated, although the *overall* deF% was at most 5% after irradiation for 48 h. Images captured before and after the reactions demonstrated that the surface of the PTFE powder, which is strongly hydrophobic, became hydrophilic and the powder sank into the aqueous solution (Supplementary Fig. S115). In other words, PTFE can be defluorinated by visible LED light although the reaction efficiency was relatively low.

Conclusion

This research showcased the efficient defluorination of PFOS and Nafion using visible LED light irradiation onto semiconductor NCs at room temperature under atmospheric pressure. Because CdS is a typical compound semiconductor and nonlinear reactions are prevalent across various compositions, this demonstrated concept has the potential for broader applicability to other low-toxicity materials. The proposed methodology is promising for the effective decomposition of diverse perfluoroalkyl substances under gentle conditions, thereby significantly contributing towards the establishment of a sustainable fluorine-recycling society.

Supporting Information

The authors have cited an additional reference within the Supporting Information.[52]

Acknowledgments

This work was supported by JST, PRESTO Grant Numbers JPMJPR22N6, JSPS KAKENHI Grant Numbers JP21K05012, JP24K01460, and Advanced Research Infrastructure for Materials and Nanotechnology, The Ultramicroscopy Research Center, Kyushu University (JPMXP1223KU0055). The authors express their gratitude to Dr. Tatsuo Nakagawa from UNISOKU Co., Ltd., for helping nanosecond to microsecond transient absorption measurements.

Keywords: semiconductor nanocrystals • nonlinear optical processes • photocatalysis • PFAS • hydrated electron

[1] L. Ahrens, M. Bundschuh, *Environ. Toxicol. Chem.* **2014**, *33*, 1921–1929.
[2] J. W. Martin, S. A. Mabury, K. R. Solomon, D. C. G. Muir, *Environ. Toxicol. Chem.* **2003**, *22*, 196–204.
[3] H. Hori, E. Hayakawa, H. Einaga, S. Kutsuna, K. Koike, T. Ibusuki, H. Kiatagawa, R. Arakawa, *Environ. Sci. Technol.* **2004**, *38*, 6118–6124.
[4] H. Hori, A. Yamamoto, E. Hayakawa, S. Taniyasu, N. Yamashita, S. Kutsuna, H. Kiatagawa, R. Arakawa, *Environ. Sci. Technol.* **2005**, *39*, 2383–2388.
[5] H. Park, C. D. Vecitis, J. Cheng, N. F. Dalleska, B. T. Mader, M. R. Hoffmann, *Photochem. Photobiol. Sci.* **2011**, *10*, 1945–1953.
[6] M. J. Bentel, Y. Yu, L. Xu, Z. Li, B. M. Wong, Y. Men, J. Liu, *Environ. Sci. Technol.* **2019**, *53*, 3718–3728.
[7] Y. Dai, X. Guo, S. Wang, L. Yin, M. R. Hoffmann, *Water Res* **2020**, *181*, 115964.
[8] L. Qian, F. D. Kopinke, A. Georgi, *Environ. Sci. Technol.* **2021**, *55*, 614–622.
[9] Z. Chen, Y. Teng, N. Mi, X. Jin, D. Yang, C. Wang, B. Wu, H. Ren, G. Zeng, C. Gu, *Environ. Sci. Technol.* **2021**, *55*, 3996–4006.
[10] J. Cui, P. Gao, Y. Deng, *Environ. Sci. Technol.* **2020**, *54*, 3752–3766.
[11] L. Duan, B. Wang, K. Heck, S. Guo, C. A. Clark, J. Arredondo, M. Wang, T. P. Senftle, P. Westerhoff, X. Wen, Y. Song, M. S. Wong, *Environ. Sci. Technol. Lett.* **2020**, *7*, 613–619.
[12] L. Chu, C. Zhang, P. Chen, Q. Zhou, X. Zhou, Y. Zhang, *J. Water Process Eng.* **2022**, *49*, 103070.
[13] B. Trang, Y. Li, X. S. Xue, M. Ateia, K. N. Houk, W. R. Dichtel, *Science* **2022**, *377*, 839–845.
[14] B. Améduri, H. Hori, *Chem Soc Rev* **2023**, *52*, 4208–4247.
[15] F. Auzel, *Chem. Rev.* **2004**, *104*, 139–173.
[16] F. Wang, X. Liu, *Chem. Soc. Rev.* **2009**, *38*, 976–989.
[17] T. N. Singh-Rachford, F. N. Castellano, *Coord. Chem. Rev.* **2010**, *254*, 2560–2573.
[18] N. Yanai, N. Kimizuka, *Chem. Commun.* **2016**, *52*, 5354–5370.
[19] Y. Kobayashi, K. Mutoh, J. Abe, *J. Photochem. Photobiol. C* **2018**, *34*, 2–28.
[20] F. Glaser, C. Kerzig, O. S. Wenger, *Angew. Chem. Int. Ed.* **2020**, *59*, 10266–10284.
[21] M. Schmalzbauer, M. Marcon, B. König, *Angew. Chem. Int. Ed.* **2021**, *60*, 6270–6292.
[22] Y. Kobayashi, J. Abe, *Chem. Soc. Rev.* **2022**, *51*, 2397–2415.
[23] M. Goez, C. Kerzig, R. Naumann, *Angew. Chem. Int. Ed.* **2014**, *53*, 9914–9916.
[24] I. Ghosh, L. Marzo, A. Das, R. Shaikh, B. König, *Acc. Chem. Res.* **2016**, *49*, 1566–1577.

[25] J. P. Cole, D. F. Chen, M. Kudisch, R. M. Pearson, C. H. Lim, G. M. Miyake, *J. Am. Chem. Soc.* **2020**, *142*, 13573–13581.
[26] F. Glaser, C. Kerzig, O. S. Wenger, *Chem. Sci.* **2021**, *12*, 9922–9933.
[27] M. Uji, T. J. B. Zähringer, C. Kerzig, N. Yanai, *Angew. Chem. Int. Ed.* **2023**, *62*, e202301506.
[28] V. I. Klimov, *J. Phys. Chem. B* **2000**, *104*, 6112–6123.
[29] C. Melnychuk, P. Guyot-Sionnest, *Chem. Rev.* **2021**, *121*, 2325–2372.
[30] Z. Deutsch, L. Neeman, D. Oron, *Nat. Nanotechnol.* **2013**, *8*, 649–653.
[31] N. S. Makarov, Q. Lin, J. M. Pietryga, I. Robel, V. I. Klimov, *ACS Nano* **2016**, *10*, 10829–10841.
[32] G. Yang, M. Kazes, D. Raanan, D. Oron, *ACS Photonics* **2021**, *8*, 1909–1916.
[33] L. R. Bradshaw, A. Hauser, E. J. McLaurin, D. R. Gamelin, *J. Phys. Chem. C* **2012**, *116*, 9300–9310.
[34] Y. Dong, J. Choi, H. K. Jeong, D. H. Son, *J. Am. Chem. Soc.* **2015**, *137*, 5549–5554.
[35] Y. Dong, D. Parobek, D. Rossi, D. H. Son, *Nano Lett.* **2016**, *16*, 7270–7275.
[36] D. Parobek, T. Qiao, D. H. Son, *J. Chem. Phys.* **2019**, *151*, 20901.
[37] J. K. Widness, D. G. Enny, K. S. McFarlane-Connelly, M. T. Miedenbauer, T. D. Krauss, D. J. Weix, *J. Am. Chem. Soc.* **2022**, *144*, 12229–12246.
[38] J. M. Mouat, J. K. Widness, D. G. Enny, M. T. Meidenbauer, F. Awan, T. D. Krauss, D. J. Weix, *ACS Catal.* **2023**, 9018–9024.
[39] Z. Alfassl, D. Bahnermann, A. Henglein, *J. Phys. Chem.* **1982**, *86*, 4656–4657.
[40] M. Haase, H. Weller, A. Henglein, *J. Phys. Chem.* **1988**, *92*, 4706–4712.
[41] Y. Han, M. Hamada, I. Y. Chang, K. Hyeon-Deuk, Y. Kobori, Y. Kobayashi, *J. Am. Chem. Soc.* **2021**, *143*, 2239–2249.
[42] W. W. Yu, L. Qu, W. Guo, X. Peng, *Chem. Mater.* **2003**, *15*, 2854–2860.
[43] H. D. Nelson, D. R. Gamelin, *J. Phys. Chem. C* **2018**, *122*, 18124–18133.
[44] T. Uchihara, T. Urasaki, T. Kamiya, Y. Tamaki, M. Ganeko, S. Kinjo, H. Oshiro, A. Kinjo, *J. Photochem. Photobiol. A* **1998**, *118*, 131–136.
[45] Horst Kisch, *Semiconductor Photocatalysis Principles and Applications*, Wiley, Weinheim, **2015**.
[46] P. E. Lippens, M. Lannoo, *Phys. Rev. B* **1989**, *39*, 10935–10942.
[47] Y. Kobayashi, T. Nishimura, H. Yamaguchi, N. Tamai, *J. Phys. Chem. Lett.* **2011**, *2*, 1051–1055.
[48] M. R. Hoffmann, S. T. Martin, W. Choi, D. W. Bahnemann, *Chem. Rev.* **1995**, *95*, 69–96.
[49] K. E. Shulenberger, H. R. Keller, L. M. Pellows, N. L. Brown, G. Dukovic, *J. Phys. Chem. C* **2021**, *125*, 22650–22659.
[50] D. Yoshioka, Y. Yoneda, I. Y. Chang, H. Kuramochi, K. Hyeon-Deuk, Y. Kobayashi, *ACS Nano* **2023**, *17*, 11309–11317.
[51] M. GutiCrrez, A. Henglein, *Ber. Bunsenges. Phy. Chem.* **1983**, *87*, 474–478.
[52] P. M. Hare, E. A. Price, C. M. Stanisky, I. Janik, D. M. Bartels, *J. Phys. Chem. A* **2010**, *114*, 1766–1775.

10.1002/anie.202408687

Entry for the Table of Contents

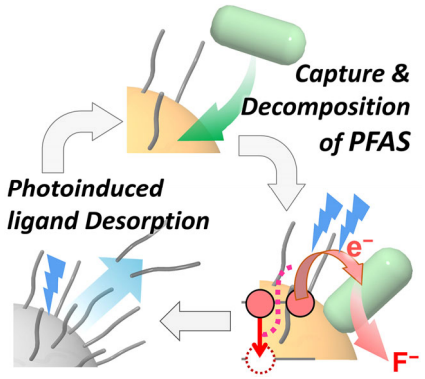

Perfluoroalkyl substances and fluorinated polymers were efficiently decomposed to fluoride ions under ambient conditions via the irradiation of visible LED light onto semiconductor nanocrystals. The decomposition is driven by cooperative mechanisms involving light-induced ligand displacements and Auger-induced electron injections via hydrated electrons and higher excited states.

Twitter/X account: @cjx91704